AMERICAN SOCIETY FOR MICROBIOLOGY | mBio

Check for updates

| Host-Microbial Interactions | Research Article

Antiviral *Wolbachia* strains associate with *Aedes aegypti* endoplasmic reticulum membranes and induce lipid droplet formation to restrict dengue virus replication

Robson K. Loterio,[1] Ebony A. Monson,[2] Rachel Templin,[3] Jyotika T. de Bruyne,[4] Heather A. Flores,[5] Jason M. Mackenzie,[6] Georg Ramm,[3] Karla J. Helbig,[2] Cameron P. Simmons,[1,4] Johanna E. Fraser[1]

AUTHOR AFFILIATIONS See affiliation list on p. 16.

ABSTRACT *Wolbachia* are a genus of insect endosymbiotic bacteria which includes strains *w*Mel and *w*AlbB that are being utilized as a biocontrol tool to reduce the incidence of *Aedes aegypti*-transmitted viral diseases like dengue. However, the precise mechanisms underpinning the antiviral activity of these *Wolbachia* strains are not well defined. Here, we generated a panel of *Ae. aegypti*-derived cell lines infected with antiviral strains *w*Mel and *w*AlbB or the non-antiviral *Wolbachia* strain *w*Pip to understand host cell morphological changes specifically induced by antiviral strains. Antiviral strains were frequently found to be entirely wrapped by the host endoplasmic reticulum (ER) membrane, while *w*Pip bacteria clustered separately in the host cell cytoplasm. ER-derived lipid droplets (LDs) increased in volume in *w*Mel- and *w*AlbB-infected cell lines and mosquito tissues compared to cells infected with *w*Pip or *Wolbachia*-free controls. Inhibition of fatty acid synthase (required for triacylglycerol biosynthesis) reduced LD formation and significantly restored ER-associated dengue virus replication in cells occupied by *w*Mel. Together, this suggests that antiviral *Wolbachia* strains may specifically alter the lipid composition of the ER to preclude the establishment of dengue virus (DENV) replication complexes. Defining *Wolbachia*'s antiviral mechanisms will support the application and longevity of this effective biocontrol tool that is already being used at scale.

IMPORTANCE *Aedes aegypti* transmits a range of important human pathogenic viruses like dengue. However, infection of *Ae. aegypti* with the insect endosymbiotic bacterium, *Wolbachia*, reduces the risk of mosquito to human viral transmission. *Wolbachia* is being utilized at field sites across more than 13 countries to reduce the incidence of viruses like dengue, but it is not well understood how *Wolbachia* induces its antiviral effects. To examine this at the subcellular level, we compared how different strains of *Wolbachia* with varying antiviral strengths associate with and modify host cell structures. Strongly antiviral strains were found to specifically associate with the host endoplasmic reticulum and induce striking impacts on host cell lipid droplets. Inhibiting *Wolbachia*-induced lipid redistribution partially restored dengue virus replication demonstrating this is a contributing role for *Wolbachia's* antiviral activity. These findings provide new insights into how antiviral *Wolbachia* strains associate with and modify *Ae. aegypti* host cells.

KEYWORDS *Wolbachia*, *Aedes aegypti*, dengue, flavivirus, antiviral, arbovirus

Arthropod-borne viruses (arboviruses) including dengue (DENV), Zika (ZIKV), chikungunya (CHIKV), and yellow fever virus (YFV) are primarily transmitted by female *Aedes aegypti* and, to a lesser extent, by female *Aedes albopictus* (1–3). The global spread of these viruses has dramatically increased in recent decades. This is largely due

Invited Editor Rushika Perera, Colorado State University, Fort Collins, Colorado, USA

Editor Nisha K. Duggal, Virginia Tech, Blacksburg, Virginia, USA

Address correspondence to Johanna E. Fraser, johanna.fraser@monash.edu.

Ebony A. Monson and Rachel Templin contributed equally to this article. Author order was determined by mutual agreement.

The authors declare no conflict of interest.

See the funding table on p. 16.

Received 13 September 2023
Accepted 20 November 2023
Published 22 December 2023

to factors associated with the geographic distribution of *Aedes* spp. such as climate change (4–7), globalization (8, 9), urbanization (9, 10), resistance to insecticides (11), and the lack of effective vector control strategies (12).

A promising biological vector control strategy that has emerged in the last decade employs antiviral strains of *Wolbachia* to restrict mosquito-to-human transmission of *Ae. aegypti*-borne viruses (13–17). *Wolbachia* is an intracellular gram-negative endosymbiotic bacterium that infects a wide range of invertebrates, including arthropods and nematodes, but it is not naturally found in *Ae. aegypti* mosquitoes (18, 19). *Wolbachia* strains can be isolated from native hosts such as *Drosophila melanogaster* (*w*Mel) (14, 20) and *Ae. albopictus* (*w*AlbB) (15, 21, 22) and then introduced into heterologous arthropods including *Ae. aegypti*. Strains such as *w*Mel and *w*AlbB induce an antiviral state in *Ae. aegypti* reducing the rate of infection, dissemination, and transmission of +RNA viruses such as DENV (14, 20, 23). *Wolbachia*'s exceptional ability to infect and alter the host germ line to facilitate their vertical transmission through the maternal lineage underpins the application of this bacterium as a biocontrol tool (14). Additionally, many *Wolbachia* strains are capable of inducing cytoplasmic incompatibility (CI), a condition that gives *Wolbachia*-carrying females a reproductive advantage (24, 25). These strains can be introgressed into wild-type *Ae. aegypti* populations to reduce their transmission potential. This approach has been shown to dramatically and significantly reduce the incidence of dengue in communities (26–31).

DENV is a member of the *Flaviviridae* family with a single positive-strand RNA genome that is surrounded by the virally encoded capsid protein in a host-derived lipid bilayer (3, 32). The viral genome is released into the host cell cytosol after entering susceptible cells via endocytosis and is translated by host machinery at the rough endoplasmic reticulum (33, 34). DENV induces drastic rearrangements of endoplasmic reticulum (ER) membranes to form viral replication complexes that are critically required to coordinate the multiple steps of viral replication, genome translation, and virion assembly (33–39). *Wolbachia*'s antiviral impacts are believed to be systemic in mosquitoes (40), but also cell autonomous whereby *Wolbachia*-infected cells do not protect surrounding *Wolbachia*-free cells from viral infection (41). At the subcellular level, viral restriction is believed to occur early before viral replication is effectively initiated (42), and low levels of progeny virus produced in the presence of *Wolbachia* have reduced infectivity (43). How *Wolbachia* induces these antiviral effects is not well understood, but a variety of hypotheses have been examined. These include competition between *Wolbachia* and viruses for nutrients and physical space within host cells (13, 44–48) and altered expression of host pro- or antiviral genes (49–52), including priming of immune pathways (23, 53, 54). Implicating the mechanisms that drive the *Wolbachia*-induced antiviral state has been difficult due to technical limitations such as failure to genetically modify *Wolbachia* and to grow it axenically. However, new experimental models may help to advance our understanding of *Wolbachia*-induced host phenotypes. Specifically, we recently found that *Wolbachia* strain *w*Pip (derived from *Culex quinquefasciatus*) does not inhibit flavivirus replication, dissemination, or transmission in *Ae. aegypti* (23, 55). We hypothesized that pairwise comparisons between *Ae. aegypti* infected with *Wolbachia* strains that do or do not induce an antiviral state may facilitate the dissociation of *Wolbachia*'s antiviral effects from the general symbiont effects. Here, we generated a unique panel of *Ae. aegypti*-derived cell lines infected with *w*Mel, *w*AlbB (the antiviral stains being utilized in *Ae. aegypti* biocontrol programs), or *w*Pip to identify the subcellular changes specifically induced by antiviral *Wolbachia* strains. We identify intimate *Wolbachia*-ER interactions and triacylglyceride biosynthesis for LD formation as key host cell modifications that contribute to the *Wolbachia*-induced antiviral state.

RESULTS

Generation of a panel of *Wolbachia*-infected *Ae. aegypti*-derived cell lines

To examine the subcellular changes specifically induced by antiviral *Wolbachia* strains, we generated a panel of *Wolbachia*-infected cell lines using the immunocompetent *Ae. aegypti*-derived cell line (*Aag2*). *Aag2* cells infected with antiviral strain *w*Mel and the *w*Mel-cured line (*w*Mel.Tet-*Aag2*) have been described previously (56). *w*AlbB-*Aag2* and *w*Pip-*Aag2* cell lines were produced by stable infection of *w*Mel.Tet-*Aag2* using *Wolbachia* isolated from previously generated cell lines (RML12-*w*AlbB) or *Ae. aegypti* eggs (Rockefeller-*w*Pip). This was done to account for insect-specific flaviviruses known to infect *Aag2* cells but not *w*Mel-*Aag2* or *w*Mel.Tet-*Aag2* (herein referred to as *Wolbachia*-free-*Aag2*) (56).

To confirm that *w*AlbB and *w*Pip had antiviral and non-antiviral impacts in these cell lines, respectively, we evaluated replication of DENV serotype 2 (DENV-2) in *Wolbachia*-free, *w*Mel-*Aag2*, *w*AlbB-*Aag2,* and *w*Pip-*Aag2* cells. Consistent with our previous findings in *Ae. aegypti* (23, 55), *w*Pip did not restrict DENV-2 replication or production of infectious virus compared to the *Wolbachia*-free line (Fig. 1A and B). Notably, *w*Pip was found to grow to a higher density than *w*Mel and *w*AlbB (average of 96 *Wolbachia* per cell, compared to 30 and 69 for *w*Mel and *w*AlbB, respectively) (Fig. 1A, in parentheses). By contrast, DENV-2 RNA copies and infectious virus were significantly reduced by *w*Mel's potent antiviral activity (approximately 3 $\log_{10}$ reduction compared to *Wolbachia*-free). *w*AlbB also significantly inhibited DENV-2 replication and infectious virus in *Aag2* cell lines, but the antiviral activity was weaker than *w*Mel (approximately 1 $\log_{10}$ reduction compared to *Wolbachia*-free). This confirms that the diverse antiviral phenotypes of *Wolbachia* strains previously demonstrated in *Ae. aegypti* mosquitoes (20, 22, 23) can be recapitulated in *Aag2* cell lines.

Antiviral *Wolbachia* strains associate with host ER membranes

Wolbachia and viruses are both obligate intracellular residents of eukaryotic cells that rely on a variety of host structures and processes to complete their life cycles. Interestingly, *Wolbachia* titers and intracellular distribution have been shown to be influenced by the host's genetic background (46, 57, 58). To gain insights into how *Wolbachia* strains may associate with *Ae. aegypti* cells to induce an antiviral phenotype, we assessed our panel of *Aag2* cell lines using transmission electron microscopy (TEM). Micrographs of the three *Wolbachia*-infected mosquito cell lines show each cell line is heavily infected with their respective *Wolbachia* strain (top row, Fig. 2A; Fig. S1). *Wolbachia* appeared similar in size and shape to mitochondria but could be differentiated by a lower electron density and an absence of cristae. We observed that antiviral strains, *w*Mel and *w*AlbB, were frequently associated with host membranes that appeared to be the host endoplasmic reticulum (ER), while the non-antiviral strain *w*Pip was not (bottom row, Fig. 2A; Fig. S1e through p). By scoring the closeness of interaction between *Wolbachia* and the ER, a striking difference was evident between antiviral and non-antiviral strains: approximately 50% of *w*Mel and *w*AlbB bacteria were in close contact with ER membranes in *Aag2* cell lines. Of those, 25% were clearly surrounded by the membranes (Fig. 2B and C). This tight association was observed in our reconstructed tomograms of *w*Mel where the bacterium was found to be surrounded by the ER double membrane and, in some instances, was wrapped multiple times (Fig. 2C—see Video S1 for the reconstructed tomogram). Meanwhile, over 75% of *w*Pip bacteria were not located near any intracellular membranes, and only 25% were situated adjacent to any part of the ER (Fig. 2B; Fig. S1m through p). To further confirm that the membrane structures were, indeed, ER, we carried out live cell imaging using an ER tracker dye which binds to the sulfonylurea receptors of ATP-sensitive K^+ channels present on ER membranes, and SYTO11 which preferentially stains *Wolbachia* DNA over eukaryote DNA (57, 59). Confocal fluorescence imaging confirmed the antiviral strains *w*Mel and *w*AlbB exhibited substantial colocalization with

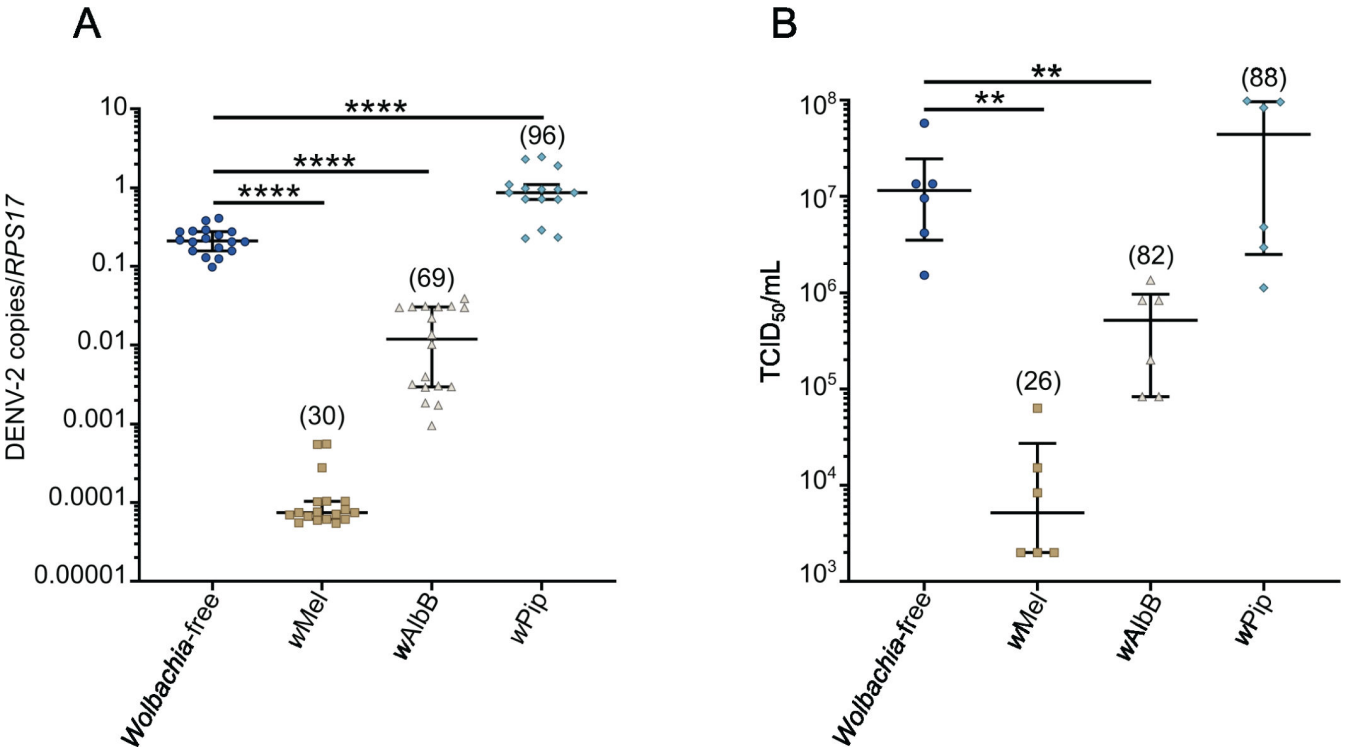

FIG 1 *w*Pip does not restrict DENV-2 replication in *Aag2* cells. *Ae. aegypti*-derived cell lines (*Aag2*) stably infected with *w*Mel, *w*AlbB, and *w*Pip strains were infected with DENV-2 at MOI 1 and compared to their matched *Wolbachia*-free line. Infectious virus and cellular RNA were collected from each cell line 7 days post-infection for analysis by tissue culture infectious dose $_{50}$ ($TCID_{50}$) and qRT-PCR. The numbers in parentheses represent the average number of *Wolbachia* per cell (*Wolbachia 16S rRNA/RPS17*), determined in parallel wells for each independent experiment prior to DENV-2 inoculation. (A) Data are the median number of virus genome copies relative to the *RPS17* mosquito housekeeping gene ±IQR. (B) Data are the median infectious viral titres ± IQR determined by $TCID_{50}$. Data are derived from at least 3 (A) or 2 (B) independent experiments performed with triplicate biological replicates each. Statistical analyses were performed using Mann-Whitney test, where $^{**}P < 0.005$, $^{****}P < 0.0001$.

ER membranes (white arrowheads, Fig. 2D), while *w*Pip did not, instead forming a massive cluster of cytosolic *Wolbachia* (Fig. 2D).

DENV and other flaviviruses significantly remodel ER membranes to form replication complexes (32, 33, 35, 36, 60). To determine whether the distinct ER interaction of antiviral *Wolbachia* strains precludes DENV-2 association with the host ER, we infected each *Aag2* cell line with DENV-2 and performed TEM analyses. We observed numerous viral replication sites containing many viral vesicle packets (Vp) in the cytosol of the *Wolbachia*-free line (white arrowheads, Fig. 2E), consistent with the high viral titers determined in this cell line (Fig. 1). We found no evidence of virus replication in any of the *w*Mel-*Aag2* cell line micrographs examined, and few and smaller Vp were observed in the *w*AlbB-*Aag2* cell line (white arrowheads, Fig. 2E). Further consistent with our data in Fig. 1, *w*Pip showed numerous Vp in the cytosol, similar to the *Wolbachia*-free control (white arrowheads, Fig. 2E). Together this data set provides the first insight into how antiviral *Wolbachia* strains differentially associate with *Ae. aegypti* ER membranes and prevent formation of typical DENV-2 replication complexes.

Antiviral *Wolbachia* strains increase lipid droplet formation in *Aag2* cells

It has previously been reported that the ER-derived organelle, lipid droplets (LDs) are upregulated following DENV infection, contributing to the cellular antiviral response in both mammalian and *Ae. aegypti*-derived cell lines (61, 62). Since the ER provides most of the constituent molecules for LDs (63), we next hypothesized that the association of antiviral *Wolbachia* strains with host ER membranes could further manipulate other intracellular lipid sources.

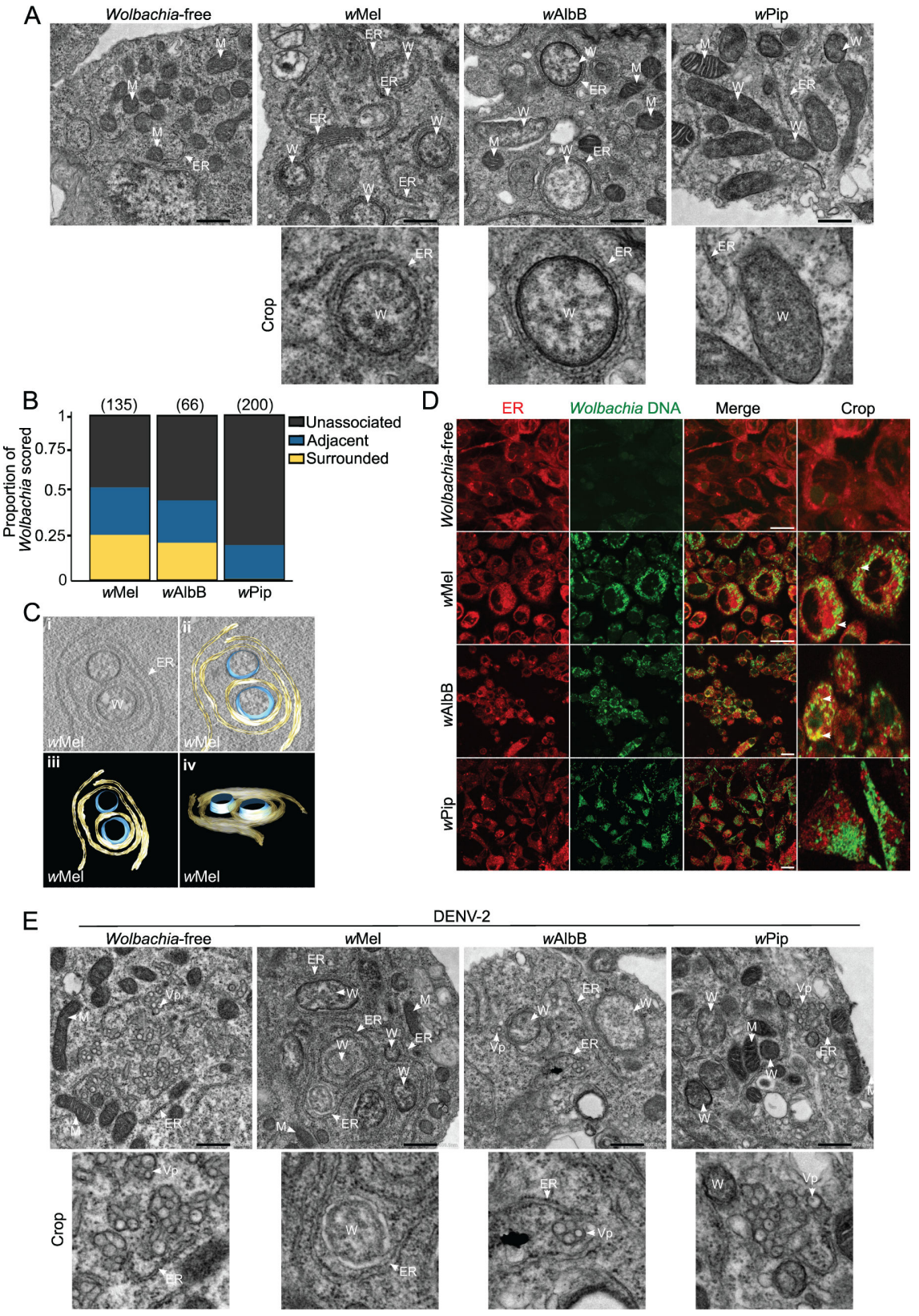

FIG 2 Antiviral *Wolbachia* strains associate with host endoplasmic reticulum membranes. (A) TEM micrographs of *Aag2* cell lines stably infected with *w*Mel, *w*AlbB, and *w*Pip show their intracellular distribution and association with ER membranes. Scale bar = 500 nm. (B) *Wolbachia*-ER interactions were manually scored as "unassociated," "adjacent," or "surrounded" from two independent experiments, where "unassociated" *Wolbachia* did not contact any host membrane,

(Continued on next page)

FIG 2 (Continued)

"adjacent" *Wolbachia* were seen to have a contact point with a host membrane but were not surrounded, and "surrounded" *Wolbachia* were entirely encompassed by a host membrane. *Wolbachia* were counted from a minimum of 28 cells in total per line. The number of *Wolbachia* bacteria scored is in parentheses. (C) TEM tomography shows *w*Mel strain surrounded by ER membranes. See Video S1 for the reconstructed tomogram. (D) Live imaging of all *Aag2* cell lines stained with SYTO 11 (*Wolbachia* DNA—green) and ER tracker (red). Scale bar = 15 µm. (E) TEM of all *Aag2* cell lines infected with DENV-2 at MOI 2 for 48 h. Scale bar = 500 nm. ER, endoplasmic reticulum; W, *Wolbachia;* M, mitochondria; Vp, vesicle packets.

To examine intracellular LDs, we stained all *Aag2* cell lines with BODIPY 493/503 and analyzed the number and size of LDs per cell. Notably, compared to the *Wolbachia*-free line, all *Wolbachia*-infected lines induced LD accumulation (Fig. 3A and B). Interestingly, *w*Mel induced the accumulation of a similar number of LD's per cell as *w*Pip (27 and 30.2 per cell, respectively), while *w*AlbB induced nearly twice the amount (50.5 per cell). However, *w*Mel-induced LDs were significantly larger than those induced by *w*AlbB and *w*Pip (791.5, 417.5, and 365.5 nm, respectively) (Fig. 3B). This implies that antiviral *Wolbachia* strains might boost the total volume of LDs per cell.

Lipid biosynthesis and degradation play a role in several stages of DENV infection, including viral replication, assembly, and energy supply (35, 64–66). Similarly, *Wolbachia* proliferation is tightly associated with changes in the host lipidome (67–69). Next, we investigated whether DENV-2 infection affected LD accumulation in the presence of each *Wolbachia* strain. In line with previous findings (61), DENV-2 induced the accumulation of LDs in *Wolbachia*-free cells (Fig. 3C and D). Interestingly, DENV-2 infection caused a further accumulation of LDs in *w*Mel-*Aag2* and *w*AlbB-*Aag2* but not in *w*Pip-*Aag2* (Fig. 3D). Furthermore, the LD accumulation observed in both cell lines with antiviral *Wolbachia* strains after DENV-2 infection was significantly higher than the LD accumulation in *Wolbachia*-free cells infected with DENV-2 (Fig. 3D). By contrast, we measured similar levels of LDs in *w*Pip- and *Wolbachia*-free *Aag2* cells infected with DENV-2 (22.5 and 21.7 per cell, respectively) (Fig. 3D), indicating an association between high LD numbers and restriction of DENV-2 replication.

To investigate LD accumulation induced by different *Wolbachia* strains *in vivo*, we dissected female *Ae. aegypti* infected with *w*Mel, *w*AlbB or *w*Pip. We selected ovarian tissue since this tissue is rich in *Wolbachia* for all strains of interest (Fig. S2) (23). Ovaries were stained with BODIPY 493/503 for LDs and DAPI to demarcate nuclei. Supporting our *in vitro* findings, LDs were most prevalent in the presence of antiviral *Wolbachia* strains compared to the *Wolbachia*-free control (Fig. 3E). Taken together, our findings demonstrate that changes in intracellular lipid storage are key features of mosquito cells infected with antiviral *Wolbachia* strains.

Intracellular redistribution of lipids contributes to DENV-2 restriction in *w*Mel-*Aag2* cells

We next hypothesized that *Wolbachia*-induced LD formation may be required to induce an antiviral state. We utilized a series of inhibitors that restrict enzymes required for LD synthesis in mammalian cells. The enzyme fatty acid synthase (FAS) catalyzes the second step of the *de novo* triacylglycerol synthesis pathway which contributes molecules to the neutral core of LDs and membrane synthesis, while diacylglycerol acyltransferase (DGAT) 1 and DGAT 2 catalyze the final step in this pathway, converting diacylglycerol to triacylglycerol (70, 71). Inhibitors of these enzymes were applied to *w*Mel- and *Wolbachia*-free-*Aag2* cells to test if they were effective against *Ae. aegypt*i orthologs. The DGAT 1 inhibitor (T863) and DGAT 2 inhibitor (PF-06424439) did not reduce LD formation in these cells. However, the fatty acid synthase (FAS) inhibitor C75 did effectively reduce LD accumulation (Fig. S3A and B).

We, therefore, compared DENV-2 replication and infectious virus production in *Wolbachia*-free and *w*Mel-*Aag2* cell lines treated with C75. We chose to focus on *w*Mel since this strain induces a more potent antiviral effect in *Aag2* cells (Fig. 1) and is the primary release strain used in field trials to date (27, 72, 73).

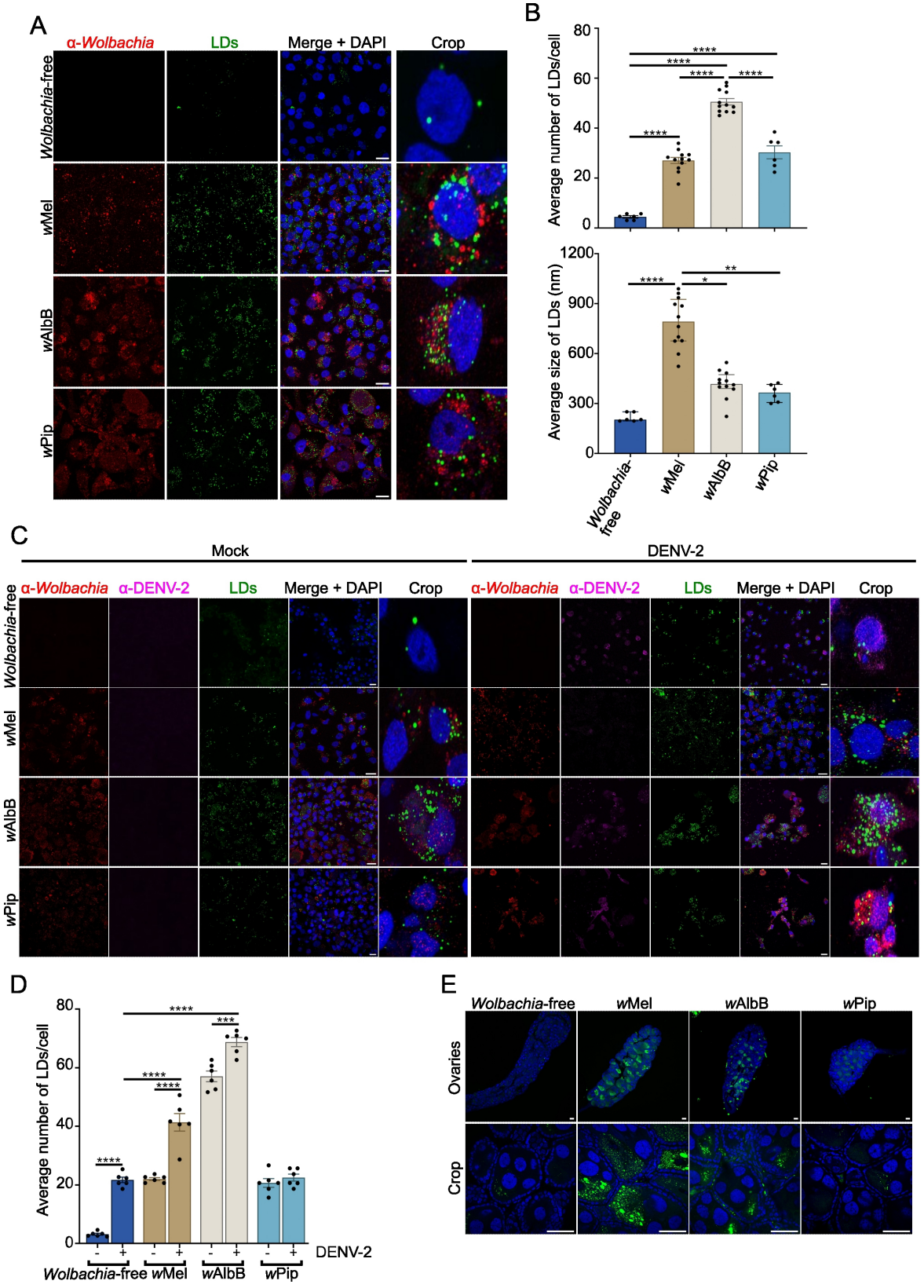

FIG 3 Antiviral *Wolbachia* strains increase lipid droplet formation in mosquito cells. (A–D) *Aag2* cells stably infected with *Wolbachia* strains *w*Mel, *w*AlbB, or *w*Pip, or *Wolbachia*-free cells were mock-infected or DENV-2 infected at MOI 1 for 24 h. (A and C) All cells were stained with BODIPY (493/503) to visualize LDs (green) and DAPI to visualize the cell nuclei (blue). *Wolbachia* was detected with an α-WSP antibody (red) and 4G2 hybridoma fluid against flavivirus group E antigen

(Continued on next page)

FIG 3 (Continued)

for DENV-2 staining (magenta). Scale bars = 15 µm. (B) LD numbers and sizes were analyzed using Fiji software. Data are the mean LD number ± SEM (top) or median LD size ± IQR (bottom) from at least 6 fields of view representing at least 80 cells in total where each data point represents the mean LD number/size from a single field of view. Data are from one experiment, representative of two independent experiments, where each experiment included triplicate biological replicates. Statistical analyses were performed by one-way ANOVA with Tukey's correction for multiple comparisons (top graph) or Kruskal-Wallis test with Dunn's correction for multiple comparisons (bottom graph), *P < 0.05, **P < 0.005, ****P < 0.0001. (D) LD numbers were analyzed using Fiji software. Data are the mean LD number ± SEM from at least 6 fields of view representing at least 80 cells in total where each data point represents the mean LD number from a single field of view. Data are from one experiment, representative of two independent experiments, where each experiment included triplicate biological replicates. Statistical analyses were performed by two-way ANOVA with Tukey's correction for multiple comparisons, *P < 0.05, **P < 0.005, ***P < 0.0005, ****P < 0.0001. (E) Ovaries were dissected from female mosquitoes 5–7 days post-emergence and stained with BODIPY (green) and DAPI (blue). Scale bars = 50 µm. All slides were imaged as 3-dimensional z-stacks and 2D images generated by Maximum Intensity Projection (MIP) using Fiji software. Images are from a single representative experiment performed on ovaries from at least three mosquitoes.

While C75 treatment reduced LD numbers in both cell lines DENV-2 replication was significantly reduced only in *Wolbachia*-free cells (by ~1 $\log_{10}$), consistent with previous reports of LDs playing a key role in DENV replication (66) (Fig. 4A , B, C and D). By contrast, C75 treatment of the *w*Mel-*Aag2* cell line partially restored DENV-2 replication, with intracellular DENV-2 and infectious virus ~1 $\log_{10}$ higher than in untreated *w*Mel-*Aag2* cells. Notably, C75 treatment of *w*Mel-*Aag2* cell lines did not reduce *Wolbachia* density (Fig. 4A and B, in parentheses), indicating that FAS and *w*Mel-induced LDs are not directly required for active *Wolbachia* replication and maintenance. However, it is possible that prolonged periods of LD depletion could affect *Wolbachia* survival.

Finally, TEM micrographs of both *Wolbachia*-free and *w*Mel-*Aag2* cell lines treated with C75 were examined to verify whether DENV-2 replication could now be supported in cells near *w*Mel bacterium. We observed a reduction in visible cytosolic Vps in the *Wolbachia*-free cell line, while, for the first time, we were able to find evidence of virus replication in cells already occupied by *w*Mel (Fig. 4E). Together, these data show that blocking the *de novo* lipogenesis of triacylglycerol significantly compromises *w*Mel-induced LD accumulation, and consequently, its antiviral activity in *Ae. aegypti* cells.

DISCUSSION

Wolbachia has been implemented as a biocontrol tool in cities in Oceania, Asia, and Latin America. Several epidemiological studies have now demonstrated the efficacy of *Wolbachia*-introgression in reducing the burden of mosquito-borne diseases in communities (26–31), and the Vector Control Advisory Group to the World Health Organization has endorsed its public health value (74). To best support the longevity of this method, and to predict the emergence of *Wolbachia*-resistant viruses, it is critical that we understand the mechanisms that underpin the antiviral activity of *Wolbachia*.

Given that *Wolbachia* strains are classified into major phylogenetic lineages known as supergroups (75), we can strategically compare host modifications induced by the antiviral strain *w*AlbB and the non-antiviral strain *w*Pip because they both belong to supergroup B. Additionally, both strains are adapted to mosquito host species (75, 76). *w*Mel, which belongs to supergroup A (75), has a well-characterized antiviral activity and comparisons with *w*AlbB enable us to determine whether antiviral strains from different supergroups employ similar strategies to induce the antiviral state in *Ae. aegypti*. In our cell culture models, we observed that supergroup B strains, *w*AlbB and *w*Pip, grew to substantially higher densities (>80 *Wolbachia*/cell) than the distantly related *w*Mel (<30 *Wolbachia*/cell). This is consistent with somatic tissues in mosquitoes where it has been reported that *w*AlbB and *w*Pip generally reside at higher levels than *w*Mel (20, 23, 55). Thus, our *in vitro* findings support previous research and show that *Wolbachia* density does not necessarily determine a strain's antiviral activity.

Recent investigations have demonstrated that *w*Mel resides nearby ER and Golgi organelles in its native host, *D. melanogaster* (46, 47, 57). Here, we remarkably observed that only antiviral *Wolbachia* strains associate closely with the ER network in *Aag2* cell lines. Non-antiviral strain *w*Pip instead formed a massive cytoplasmatic cluster with no

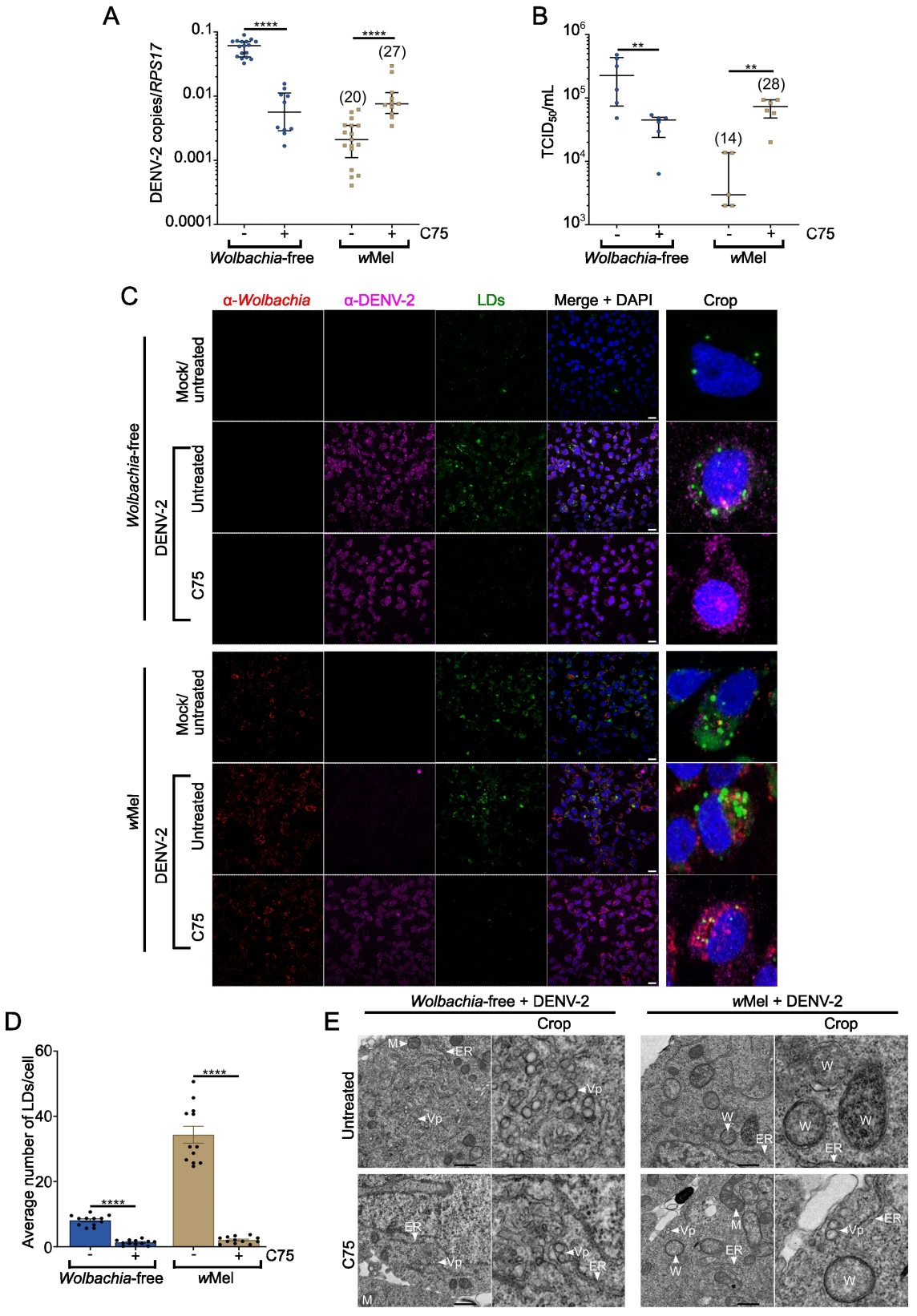

FIG 4 Disrupting *Wolbachia*-induced lipid droplets facilitates viral replication in *w*Mel-*Aag2* cell line. *Wolbachia*-free and *w*Mel-*Aag2* cell lines were mock-infected or DENV-2 infected at MOI 1 for 24 h. Prior to DENV-2 infection cells were pre-treated with C75 for 24 h, and C75 was maintained during the time of infection. (A–B) Cell-associated RNA and virus supernatant were collected from each cell line 24 h post-DENV-2-infection for analysis by qRT-PCR (A) and $TCID_{50}$ (B). Data

(Continued on next page)

FIG 4 (Continued)

are the median number of viral genome copies ± IQR relative to the *RPS17* mosquito housekeeping gene (A) or the median $TCID_{50}$/mL ± IQR (B). The numbers in parentheses represent the average number of *Wolbachia* per cell (*Wolbachia 16S rRNA/RPS17*), determined in parallel wells for each independent experiment prior to DENV-2 inoculation. Data are representative of at least three (A) or two independent experiments (B) with triplicate biological replicates each. Statistical analyses were performed using Mann-Whitney test, where $^{**}P < 0.001$ and $^{****}P < 0.0001$. (C) *Wolbachia*-free (top panel) and *w*Mel-*Aag2* cell lines (bottom panel) were stained with BODIPY (green) and DAPI (blue). *Wolbachia* was detected with an α-WSP antibody (red) and 4G2 hybridoma fluid against flavivirus group E antigen for DENV-2 staining (magenta). Slides were imaged as 3-dimensional z-stacks and 2D images generated by MIP using Fiji software. Scale bars = 15 µm. (D) LD numbers were quantified 24 h post-DENV-2 infection at MOI 1. LD numbers were analyzed using Fiji software. Data are the mean LD number ± SEM from at least 6 fields of view representing at least 80 cells in total, where each data point represents the mean LD number from a single field of view. Statistical analyses were performed by an unpaired two-tailed student's *t*-test, where $^{****}P < 0.0001$. (E) TEM of *Wolbachia*-free and *w*Mel-*Aag2* cell lines mock-infected or DENV-2 infected at MOI 1 for 24 h and treated with C75 as previously described. Scale bar = 500 nm. ER, endoplasmic reticulum; W, *Wolbachia*; M, mitochondria; Vp, vesicle packets.

apparent interaction with other organelles. TEM analyses revealed that *w*Mel and *w*AlbB were individually surrounded by ER membranes at a high frequency. This may be strategic by these strains; for example, the *w*Mel genome lacks pathways for metabolizing some membrane components, relying on its host for many of the materials required for their membrane formation (77–79). Since *w*Pip does not demand this close association for its active replication, perhaps it has alternate ways of acquiring nutrients or has a more complete intrinsic metabolic capacity. Comparative genomic studies between related strains *w*AlbB and wPip may provide insight into this. Interestingly, based on our TEM micrographs, even in *Aag2* cell lines highly infected with *w*AlbB or *w*Pip strains (>80 *Wolbachia*/cell), we did not see any morphological evidence of increased ER activity linked to ER stress, such as enlarged tubules and cisternae, nor subcellular redistribution of this organelle as previously described for *w*Mel in *D. melanogaster* (46, 47).

To our knowledge, there have not been any reports describing the association of *Wolbachia* strains with *Ae. aegypti* organelles using sectioned mosquitoes or dissected tissues. Such an examination will be important to confirm the *in vivo* relevance of the findings described here. Notably, *w*Mel and *w*AlbB are known to reside at varying density throughout a variety of *Ae. aegypti* tissues. This includes tissues known to be important for transmission of DENV like the salivary glands (80). Thus, intracellular modification of organelles in these tissues could conceivably affect the potential for these tissues to support viral replication.

DENV and other flaviviruses considerably remodel ER membranes for their own replication (32, 33, 35, 36, 60). While it is interesting that only the antiviral *Wolbachia* strains were found to be substantially associated with this organelle, our TEM analyses did not indicate any spatial competition between antiviral *Wolbachia* strains and DENV-2 for ER membranes. Indeed, ER membranes are prolific in eukaryotic cells and we observed large regions of *Aag2* cells that had ER membranes free from *Wolbachia*, with space to hypothetically support formation of viral replication complexes. Instead, we hypothesize that antiviral *Wolbachia* strains may biochemically alter the composition of the ER membranes in *Aag2* cells by eliciting the formation of LDs. LDs may then have further direct or indirect roles in mediating viral restriction.

LDs are thought to have conflicting roles in viral infection: many reports have demonstrated that enveloped viruses usurp LDs and alter lipidomic profiles of host cells to enhance their viral life cycles, with lipids accounting for 20%–30% of the weight of the virion (61, 66, 81–85). DENV infection, for example, increases LD formation (61), recruiting FAS to the virus replication site (64), and its capsid protein accumulates on the surface of LDs, facilitating viral replication by providing a platform for nucleocapsid formation during encapsidation (66). By contrast, LDs have been shown to have a critical role in supporting innate immune signaling pathways, potentially acting as a platform to augment and coordinate the cell's antiviral response (61, 62, 86, 87). Since recent studies have suggested that *Wolbachia*'s antiviral activity toward DENV is not driven by innate immune priming (23, 53), it remains unclear what role *Wolbachia*-induced LDs may have in viral restriction.

In this study, we noticed distinct LD profiles in *Aag2* single-infected with *Wolbachia* strains. Antiviral *Wolbachia* strains induced a higher volume of LDs per cell than *w*Pip. Additionally, we found that *w*Mel- and *w*AlbB-*Aag2* cell lines responded to DENV-2 infection by further accumulating LDs, which did not occur in *w*Pip-*Aag2* cell line. Based on these findings, it appears that DENV-2 replication in *Aag2* cell lines requires a preferred LD accumulation threshold that, if crossed, e.g., in the presence of antiviral *Wolbachia* strains, no longer supports DENV-2 replication. Previously, *Aag2* cells infected with *w*MelPop (a supergroup A pathogenic antiviral *Wolbachia* strain from *D. melanogaster*) were shown to have LDs enriched in esterified cholesterol. DENV-2 replication was partially rescued in these cells by dispersing localized cholesterol using the drug 2-hydroxypropyl-β-cyclodextrin. However, this phenotype was not reproducible in *Ae. albopictus*-derived cells, *Aa23*, infected with another supergroup A antiviral *Wolbachia* strain, *w*Au (88, 89). Therefore, assessment of all antiviral strains using a common approach will be important in the future to determine whether some antiviral strains utilize different antiviral mechanisms in *Ae. aegypti*.

Meanwhile, Manokaran and colleagues discovered that acyl-carnitines (intermediate molecules that transport activated fatty acids, FA-CoA, from the cytoplasm to the mitochondria) are downregulated in the presence of *w*Mel, re-directing lipid sources from β-oxidation, and negatively affecting ATP production, which is required for efficient DENV-1 and Zika virus replication (48). All these findings support our hypothesis that antiviral *Wolbachia* strains affect essential lipid classes and limit their availability to sustain DENV replication.

C75 inhibition of LD formation has previously been shown to impact DENV-2 RNA replication in the absence of *Wolbachia*. This is thought to be because C75 treatment would disrupt localization of the capsid protein at host LDs (66, 90). Here, C75 treatment of *w*Mel-*Aag2* cells abrogated LD formation and instead supported an increase in intracellular and infectious titers of DENV-2, to levels comparable with C75-treated *Wolbachia*-free-*Aag2* cells. This supports a model whereby excess LD's induced by *w*Mel have a strong antiviral role, while moderate levels of LDs have a pro-viral role (as seen in *Wolbachia*-free *Aag2* cells), and LD abrogation leads to incomplete viral restriction (as we observed in both *w*Mel- and *Wolbachia*-free *Aag2* cells treated with C75). While C75 effectively reduced LD numbers in *Wolbachia*-free and *w*Mel-*Aag2* cells, DGAT1 and 2 inhibitors did not. This is most likely due to a lack of conservation of these enzymes, or the inhibitor binding sites between mammalian and *Ae. aegypti* orthologs.

It is important to acknowledge that the C75 target, FAS, does not directly drive formation of LDs, and instead catalyses synthesis of triacylglycerols. Excess free fatty acids are converted into neutral lipids and stored in cytosolic LDs. Primarily, FAS synthesizes palmitate from acetyl-CoA and malonyl-CoA in the presence of NADPH (71). Thus, although FAS inhibition was associated with reduced LD formation, we cannot exclude the possibility that other FAS-mediated changes in fatty acid homeostasis are responsible for the partial restoration of DENV-2 replication in *w*Mel-*Aag2* cells.

One impact of reducing LD formation is the accumulation of lipids at ER membranes, especially precursors of triacylglycerols and sterol esters (such as cholesterol), which constitute most of the structural core of LDs (91, 92). Within the several classes of lipids, sphingolipids and sterols are essential in determining membrane flexibility and stability (93, 94). Therefore, an adequate membrane-lipid composition in the ER is critical for membrane rearrangement and assembly and function of +RNA virus replication complexes (32, 33, 35, 36, 60). Thus, the reduction of LD formation following C75 treatment might facilitate DENV-2 acquisition of lipid classes in the ER that may not normally be available in the presence of antiviral *Wolbachia* strains. Moreover, dysregulation of LDs could modify not only the composition of the ER membranes but also the composition of the LDs, both of which are required for DENV replication. In reality, *Wolbachia*'s redistribution of lipids within cells may mask intracellular competition for lipids. That is, differential localization of specific lipid classes that prevent effective viral replication on ER membranes may not have been detected in past lipidomic studies if

the overall prevalence of each lipid class remains the same (48, 69). The mechanism by which antiviral *Wolbachia* strains remove lipids from ER membranes and store them as LDs must therefore be further examined.

These results provide the first detailed analyses of how antiviral *Wolbachia* strains associate with and modify *Ae. aegypti* cell organelles to restrict viral replication. We identify two striking phenotypes induced only by antiviral strains, including intimate association with host ER membranes, and induction of bigger and/or more numerous LDs. Our data support a role for *Wolbachia*-induced lipid redistribution in restriction of DENV-2 replication.

MATERIALS AND METHODS

Cell line generation and maintenance *w*Mel-*Aedes aegypti*-derived (*Aag2*) cell line and the *Wolbachia*-free *w*Mel.Tet-*Aag2* cell lines have been described previously (56). Briefly, *w*Mel.Tet-*Aag2* was generated by treating *w*Mel-*Aag2* cell line with 10 µg/mL tetracycline for three successive passages, to cure the line of *w*Mel infection. This *Wolbachia*-free-*Aag2* cell line was then further used to generate *w*AlbB-*Aag2* and *w*Pip-*Aag2* cell lines. *w*AlbB strain was purified from the *Ae. albopictus*-derived cell line, RML-12, stably infected with *w*AlbB and infection of *Wolbachia*-free-*Aag2* cells was done using the shell vial technique as described previously (58).

To generate *w*Pip-*Aag2*, *w*Pip was extracted from infected *Ae. aegypti* eggs (95). In an Eppendorf tube, 1,000–2,000 2- to 5-day-old eggs were rinsed 3–5 times in 1 mL distilled water. The eggs were passed through a 100 µm mesh sieve and placed in a new Eppendorf tube containing 1 mL 80% (vol/vol) ethanol. Eggs were sterilized by 3–5 washes in 80% (vol/vol) ethanol then rinsed three times in distilled water, sieved, and transferred to a new Eppendorf tube containing 500 µL SPG buffer (218 mM sucrose, 3.8 mM KH_2PO_4, 7.2 mM K_2HPO_4, 4.9 mM L- glutamate at pH 7.4). Eggs were rinsed three times in SPG buffer then homogenized in 300–500 µL SPG buffer using a plastic pestle. The homogenate was spun to remove debris, and the supernatant was collected in a fresh tube. This was repeated three to five times until the supernatant became clear. A pool of supernatant samples was created. Under sterile conditions, the *w*Pip-containing supernatant was then passed through a 5-µm syringe filter followed by a 2.7-µm syringe filter. The filtrate was then centrifuged at 12,000 *g* to pellet *Wolbachia*. Extracted *w*Pip pellet was finally resuspended in ~300 µL of sterile SPG buffer. *Wolbachia*-free-*Aag2* cell line was then infected with the purified *w*Pip using the shell vial technique (58).

All *Aag2* cell lines (hereafter referred as *Wolbachia*-free-*Aag2*, *w*Mel-*Aag2*, *w*AlbB-*Aag2*, and *w*Pip-*Aag2* cell lines) were routinely cultured at 26°C in maintenance media consisting in 1:1 Schneider's Drosophila (Gibco)/Mitsuhashi and Maramorosch [$CaCl_2$ 0.151 g/L, $MgCl_2$ 0.047 g/L, KCl 0.2 g/L, NaCl 7 g/L, NaH_2PO_4 0.174 g/L, D(+)-glucose 4 g/L, yeast extract 5 g/L, lactalbumin hydrolysate 6.5 g/L, and $NaHCO_3$ 0.12 g/L at pH 6.9] medium supplemented with 10% fetal bovine serum (FBS—Gibco).

C6/36 cell lines of *Aedes albopictus* origin were supplied by the American Type Culture Collection (ATCC) were routinely cultured at 28°C with 5% CO_2 in RPMI 1640 medium (Gibco) with GlutaMAX Supplement containing 10% FBS.

Wolbachia density

Wolbachia density was routinely monitored in each cell line. To determine the average number of *Wolbachia* per cell, we used qPCR to measure the relative abundance of the conserved *Wolbachia 16S rRNA* gene to that of the single-copy mosquito house-keeping gene *RPS17* gene. *Wolbachia*-free cells and *w*Mel-, *w*AlbB-, and *w*Pip-*Aag2* cell lines were lysed with squash extraction buffer [10 mM Tris Buffer, 1 mM ethylenediamine tetraacetic acid (EDTA), 50 mM NaCl in ultrapure water, 1:50 Proteinase K]. Cell lysates were then incubated at 56°C for 5 min, followed by 98°C for 5 min. Samples were diluted 1:10 in water, and qPCR was performed with 3 µL of each diluted cell lysate using the LightCycler 480 Probes Master mix (Roche) according to the manufacturer's instructions. Probes

and primers used are as described: For *Wolbachia* detection, *16S rRNA* F (5′-GAGTGA AGAAGGCCTTTGGG-3′), *16S rRNA* R (5′-CACGGAGTTAGCCAGGACTTC-3′), and *16S rRNA* Cy5 probe (5′-LC640CTGTGAGTACCGTCATTATCTTCCTCACT-IowaBlackRQ-3′) were used. To detect the housekeeping gene, *RPS17* F (5′-TCCGTGGTATCTCCATCAAGCT-3′), *RPS17* R (5′-CACTTCCGGCACGTAGTTGTC-3′), and *RPS17* FAM probe (5′FAM- CAGGAGGAGGAACGT GAGCGCAG-BHQ1-3′) were utilized. PCR cycling conditions were 95°C for 5 min, 45 cycles of 95°C for 10 s, 60°C for 15 s, 72°C for 1 s, followed by cooling at 40°C for 10 s. *Wolbachia* densities were quantified using the delta CT method ($2^{CT(reference)}$/ $2^{CT(target)}$) (96).

DENV-2

Dengue virus serotype 2 (DENV-2) strain 92T (isolated from human serum collected from a patient from Townsville, Queensland/Australia, in 1992) (13) was prepared by inoculation of C6/36 cell lines with a multiplicity of infection (MOI) of 0.1 and collection of culture supernatant 13–14 days post-infection. Infectious titers were determined by $TCID_{50}$.

DENV-2 infection of cell lines

Aag2 cell lines were seeded to reach 90% confluency in 24, 12, or 6 well-plates and incubated at 26°C for 48 h prior to viral infection. Unless otherwise stated, cells were infected with DENV-2 at MOI 1 in maintenance medium without FBS for 2 h at 26°C. Virus inoculum was then removed, and the cells were washed once with warm PBS. Maintenance media containing 2% FBS were added, and cells were then incubated at 26°C for the indicated time.

Quantification of DENV-2 RNA

To quantify DENV-2 genomic copies, total RNA from virus-infected cells was extracted using the RNeasy kit (Qiagen) or Isolate II RNA mini kit (Bioline). DENV-2 RNA was amplified by qRT-PCR (LightCycler Multiplex RNA Virus Master, Roche), using primers to the conserved 3′UTR: Forward 5′-AAGGACTAGAGGTTAGAGGAGACCC; Reverse 5′- CGTTC TGTGCCTGGAATGATG; Probe 5′-HEX- AACAGCATATTGACGCTGGGAGAGACCAGA-BHQ13′ (23); DENV-2 RNA copies were quantified relative to *Ae. aegypti* house-keeping gene *RPS17* (primers and probe sequences as above) using the delta CT method ($2^{CT(reference)}$/ $2^{CT(target)}$) (96). Reactions were run on a LightCycler 480 (Roche), and data analysis was carried out with the LightCycler 480 software. qRT-PCR conditions: 50°C for 10 min, 95°C for 30 s, followed by 45 cycles of 95°C for 10 s, 55°C for 5 s, and 72°C for 10 s.

Tissue culture infectious dose $_{50}$ ELISAs to determine viral titres

Infectious virus levels were determined by Tissue Culture Infectious Dose $_{50}$ ($TCID_{50}$) as previously described (97). Briefly, serial dilutions (10-fold) of virus were inoculated onto C6/36 cell lines in flat-bottom 96 well plates containing maintenance medium (RPMI-1640, 2% FBS) and incubated for 13–14 days at 28°C. After the incubation period, media were aspirated, and cells were fixed with acetone fixative buffer (20% acetone/0.02% BSA in PBS) at 4°C for 24 h. The fixative was removed, and the plate was left to completely air-dry. Once dried, virus concentrations were immediately quantified by ELISA or plates were kept at –20°C until required.

ELISAs were performed using monoclonal antibody 4G2 to detect DENV E protein (98). Briefly, plates were blocked with 2% casein in TNE buffer (10 mM Tris; 0.2 M NaCl; 1 mM EDTA; 0.05% Tween20) for 1 h at room temperature. 4G2 (produced as hybridoma supernatant) (99) was diluted 1:200 in blocking solution and incubated on fixed cells for 1 h at 37°C. Plates were washed four times with PBST (0.05% Tween20). Anti-mouse secondary antibody was diluted 1:2,000 in blocking solution and incubated for 1 h at 37°C. Plates were washed six times with PBST and then incubated with 3,3′5,5′-tetramethylbenzidine (TMB) for up to 5 min. The reaction was stopped by the addition of 0.1 M HCl. The absorbance of each well was measured at 450 nm using a BioTek Gen5

microplate reader (Agilent, Santa Clara, CA, USA). The $TCID_{50}$/mL was determined using the Reed-Muench calculation (100).

Cell fixation and processing for transmission electron microscopy

Aag2 cell lines were seeded in a 6-well cell culture plate in triplicate at a concentration of 3×10^6 cells/well for 48 h at 26°C. Unless otherwise stated, cells were mock-infected or infected for 2 h at 26°C with DENV-2 at MOI 2 in maintenance media without FBS. Virus inoculum was then removed, and cells were washed once with warm PBS. Maintenance media containing 2% FBS were added, and cells were incubated at 26°C for 2 days. For C75 treatment, cells were treated as described below and infected with DENV-2 at MOI 1. At 24 h post-infection, cells were washed once with warm PBS and fixed for 2 h at room temperature with 2% glutaraldehyde in 0.1 M sodium cacodylate buffer. Cells were gently washed three times for 10 min each with 0.1 M sodium cacodylate buffer.

Cells were post fixed in 1% osmium tetroxide in 0.1 M sodium cacodylate buffer for 30 min at room temperature which was then reduced with 1.5% potassium ferrocyanide in 0.1 M sodium cacodylate buffer for 30 min. Cells were washed three times for 10 min with ultrapure water. Staining with 2.5% uranyl acetate (aqueous) followed overnight at 4°C. Cells were once again washed 3 times for 10 minutes with ultrapure water. Following washing, cells were scraped and pelleted into 4% agarose in water. Pellets were dehydrated with increasing concentrations of ethanol (25%, 50%, 75%, 90%, 100%, 100%) followed by acetone (100%, 100%). Each dehydration step was aided by a microwave regime of 40 s at 150 W (Pelco Biowave). Pellets were infiltrated with epon resin using a microwave regime (25%, 50%, 75%, 100%, 100%; each step 3 min at 250 W under vacuum). Pellets were transfered to fresh 100% epon and left at room temperature overnight and finally embedded in a silicone mold for polymerization for 48 h at 60°C.

Transmission electron microscopy

Seventy nanometer of sections were cut on a ultramicrotome (Leica UC7) and collected on copper mesh grids. Transmission electron microscopy (TEM) imaging was conducted on a Jeol JEM1400-Plus at 80 kV. A combination of single snapshots and image montages was acquired; montages were automatically stitched by Jeol acquisition software (TEM Centre).

Electron tomography

Two hundred nanometer of sections were collected on copper mesh grids for electron tomography. Ten nanometer gold fiducials were added to both sides of the section. Single-axis tomography was performed on a Jeol JEM1400-Plus at 120 kV using Jeol Recorder software. Tilt series were recorded with tilt angles from +65° to −65° with varying tilt increments based on a Saxton scheme. IMOD software (101) was used to reconstruct tilt series (etomo package), manual segmentation, and visualization.

Immunofluorescence analyses

Live experiments

Cells were plated on 18 mm × 18 mm coverslips in a 6-well cell culture plate 48 h previously coated with gelatin (0.2%, vol/vol) (62, 86). To stain the ER, the cell culture medium was aspirated, and cells were washed with PBS once and incubated for 30 min at 26°C with 1 µM live ER-tracker red dye (Molecular Probes) diluted in the appropriate *Aag2* cell culture medium. The ER-tracker solution was replaced by a 1/20,000 solution of SYTO-11 (Molecular Probes) DNA dye for 10 min at 26°C diluted in the appropriate *Aag2* cell culture medium, washed twice with PBS, and cells were maintained in *Aag2* culture medium during the confocal microscopy observations.

LDs staining and quantification

Cells were plated on 12 mm × 12 mm coverslips in a 12-well cell culture plate for 48 h previously coated with gelatin (0.2%, vol/vol) (62, 86). All cells were maintained in *Aag2* cell culture medium with 10% FBS. Twenty-four hours post-DENV-2-infection, mock-infected and infected cells were fixed with 4% paraformaldehyde in PBS for 15 min, washed twice with PBS, permeabilized with 0.5% Saponin in PBS for 10 min, and washed three times with PBS. Cells were blocked with 5% BSA for 1 h, before antibody staining with polyclonal anti-WSP (98) and 4G2 hybridoma fluid against flavivirus group E antigen for DENV-2 staining. Cells were then incubated with Alexa Fluor 555 or 647 secondary antibodies (1:2,000) for 1 h. LDs were stained by incubating cells with BODIPY (493/503 4,4-difluoro 1,3,5,7,8 pentamethyl 4-bora3a,4a-diaza-s-indacene—Molecular Probes) at 1 ng/mL for 1 h, and nuclei were stained with DAPI (Sigma-Aldrich, 1 µg/mL) for 5 min. All incubations were at room temperature. Samples were then washed with PBS and mounted with Vectashield Antifade Mounting Medium (Vector Laboratories). The slides were imaged as 3-dimensional z-stacks and 2D images generated by Maximum Intensity Projection (MIP). For each condition, at least 6 fields of view were imaged at 63× magnification from different locations across each coverslip. LDs from at least 80 cells per biological replicate with a minimum of 2 biological replicates per experiment being analyzed for both LD number and average LD size. LD numbers and diameters were analyzed using quantitative data from the single raw CZI images (from Zen Blue) in ImageJ using the particle analysis tool.

For imaging of mosquito tissues, ovaries were dissected from non-blood-fed female mosquitoes 5–7 days post-emergence. Mosquito lines Rockefeller, Rockefeller-*w*Mel, Rockefeller-*w*AlbB, and Rockefeller-*w*Pip have been described previously (23). Ovaries were dissected from 4 to 5 mosquitoes per line, in PBS, then fixed on poly-lysine coated slides in cold 4% paraformaldehyde/PBS for 15 min. Slides were rinsed three times in PBS and then permeabilized in 0.1% Triton X-100 in PBS for 10 min. Samples were blocked with 1% BSA for 30 min and then stained with BODIPY (493/503) at 1 ng/mL for 1 h. Nuclei were stained with DAPI (Sigma-Aldrich, 1 µg/mL) for 5 min at room temperature. Samples were washed with PBS and mounted with Vectashield Antifade Mounting Medium (Vector Laboratories). All images were acquired using a Zeiss LSM 800 confocal microscope and processed using Zeiss analysis software (Zen Blue Edition version 10.1.19043, Jena, Germany) and FIJI analysis software. The slides were imaged as 3-dimensional z-stacks and 2D images generated by MIP.

Inhibition of FAS by C75 treatment

Unless otherwise stated, *Wolbachia*-free and *w*Mel-*Aag2* lines were seeded and infected as described above. Prior to DENV-2 infection cells were pre-treated with 1µM fatty acid synthase (FAS) inhibitor C75 (Abcam) or DMSO diluent only for 24 h. Cells were mock-infected or DENV-2-infected at MOI 1 for 24 h, and C75 was maintained during the time of infection in *Aag2* cell culture medium with 10% FBS. LD quantification, viral replication, and TEM imaging were performed as described above.

Statistical analyses

Statistical analyses of parametric data were performed using one-way ANOVA or two-way ANOVA tests with a Tukey's multiple comparison correction, or unpaired two-tailed Student's *t* test, and data were expressed as mean ± Standard Error of the Mean (±SEM). Statistical analyses of non-parametric data were performed using a Kruskal-Wallis test with Dunn's correction for multiple comparisons, or a two-tailed Mann-Whitney test, and data were expressed as median ± Interquartile Range (± IQR). All statistical analyses were performed using Prism 9.3.1 (GraphPad Software), with $P < 0.05$ considered to be significant.

ACKNOWLEDGMENTS

This research was funded by the Australian Research Council (DP220102997) and the National Health and Medical Research Council (APP1182432). The funders had no role in study design, data collection, and interpretation, or the decision to submit the work for publication.

We thank Professor Roy Hall and Jody Hobson-Peters (University of Queensland) for provision of the 4G2 antibody.

The authors would like to acknowledge the Ramaciotti Centre for Cryo Electron Microscopy, a node of Microscopy Australia. The authors acknowledge Monash Micro Imaging, Monash University, for the provision of instrumentation, training, and technical support. We would like to thank the La Trobe University Bioimaging Facility for their assistance with image acquisition, data collection, and image analysis essential to this work. Finally, we thank Katrina Ibay for technical support.

R.K.L. performed the majority of the experiments; E.A.M. assisted in the design of LD experiments, LD imaging, and image analyses. R.T. and G.R. assisted with the T.E.M. acquisition. E.A.M. and R.T. equally collaborated to this work. J.T.B. originally established wPip-Aag2 and wAlbB-Aag2 mosquito cell lines, and H.F. kindly provided the mosquito lines used in this study. J.M., K.J.H., and C.P.S. assisted in experimental direction. J.E.F. was responsible for the overall study design, alongside R.K.L. J.E.F. J.M.M. and C.P.S. acquired the funding for the project. J.E.F. and R.K.L. wrote the manuscript; all authors contributed to editing of the manuscript.

AUTHOR AFFILIATIONS

[1]Department of Microbiology, Biomedicine Discovery Institute, Monash University, Clayton, Australia
[2]Department of Microbiology, Anatomy, Physiology and Pharmacology; School of Agriculture, Biomedicine and Environment, La Trobe University, Melbourne, Australia
[3]Ramaciotti Centre For Cryo-Electron Microscopy, Monash University, Clayton, Australia
[4]World Mosquito Program, Monash University, Clayton, Australia
[5]School of Biological Sciences, Monash University, Clayton, Australia
[6]Department of Microbiology and Immunology, University of Melbourne at the Peter Doherty Institute for Infection and Immunity, Melbourne, Australia

AUTHOR ORCIDs

Robson K. Loterio http://orcid.org/0000-0002-8645-5158
Jason M. Mackenzie http://orcid.org/0000-0001-6613-8350
Johanna E. Fraser http://orcid.org/0000-0002-8020-2985

FUNDING

Funder	Grant(s)	Author(s)
Department of Education and Training | Australian Research Council (ARC)	DP220102997	Johanna E. Fraser Cameron P. Simmons Jason M. Mackenzie
DHAC | National Health and Medical Research Council (NHMRC)	APP1182432	Johanna E. Fraser Cameron P. Simmons

AUTHOR CONTRIBUTIONS

Robson K. Loterio, Data curation, Formal analysis, Methodology, Writing – original draft, Writing – review and editing | Ebony A. Monson, Data curation, Formal analysis, Writing – review and editing | Rachel Templin, Data curation, Formal analysis, Writing – review and editing | Jyotika T. de Bruyne, Data curation, Resources, Writing – review and editing | Heather A. Flores, Resources, Writing – review and editing | Jason M. Mackenzie,

Methodology, Writing – review and editing | Georg Ramm, Resources, Supervision, Writing – review and editing | Karla J. Helbig, Supervision, Writing – review and editing | Cameron P. Simmons, Supervision, Writing – review and editing | Johanna E. Fraser, Conceptualization, Formal analysis, Funding acquisition, Resources, Supervision, Writing – original draft, Writing – review and editing

ADDITIONAL FILES

The following material is available online.

Supplemental Material

Supplemental material (mBio02495-S0001.docx). Supplemental text, figures, movie legend, and references.
Video S1 (mBio02495-S0001.avi).

REFERENCES

1. Ogunlade ST, Meehan MT, Adekunle AI, Rojas DP, Adegboye OA, McBryde ES. 2021. A review: *Aedes*-borne arboviral infections, controls and *Wolbachia*-based strategies. Vaccines 9:32. https://doi.org/10.3390/vaccines9010032
2. Weaver SC, Barrett ADT. 2004. Transmission cycles, host range, evolution and emergence of arboviral disease. Nat Rev Microbiol 2:789–801. https://doi.org/10.1038/nrmicro1006
3. Mukhopadhyay S, Kuhn RJ, Rossmann MG. 2005. A structural perspective of the flavivirus life cycle. Nat Rev Microbiol 3:13–22. https://doi.org/10.1038/nrmicro1067
4. Kraemer MUG, Reiner RC, Brady OJ, Messina JP, Gilbert M, Pigott DM, Yi D, Johnson K, Earl L, Marczak LB, et al. 2019. Past and future spread of the arbovirus vectors *Aedes aegypti* and *Aedes albopictus*. Nat Microbiol 4:854–863. https://doi.org/10.1038/s41564-019-0376-y
5. Brady OJ, Golding N, Pigott DM, Kraemer MUG, Messina JP, Reiner Jr RC, Scott TW, Smith DL, Gething PW, Hay SI. 2014. Global temperature constraints on *Aedes aegypti* and *Ae. albopictus* persistence and competence for dengue virus transmission. Parasit Vectors 7:338. https://doi.org/10.1186/1756-3305-7-338
6. Ryan SJ, Carlson CJ, Mordecai EA, Johnson LR. 2019. Global expansion and redistribution of *Aedes*-borne virus transmission risk with climate change. PLOS Negl Trop Dis 13:e0007213. https://doi.org/10.1371/journal.pntd.0007213
7. Goindin D, Delannay C, Ramdini C, Gustave J, Fouque F. 2015. Parity and longevity of *Aedes aegypti* according to temperatures in controlled conditions and consequences on dengue transmission risks. PLOS ONE 10:e0135489. https://doi.org/10.1371/journal.pone.0135489
8. Morens DM, Folkers GK, Fauci AS. 2004. The challenge of emerging and re-emerging infectious diseases. Nature 430:242–249. https://doi.org/10.1038/nature02759
9. Kraemer MUG, Sinka ME, Duda KA, Mylne A, Shearer FM, Brady OJ, Messina JP, Barker CM, Moore CG, Carvalho RG, Coelho GE, Van Bortel W, Hendrickx G, Schaffner F, Wint GRW, Elyazar IRF, Teng H-J, Hay SI. 2015. The global compendium of *Aedes aegypti* and *Ae. albopictus* occurrence. Sci Data 2:150035. https://doi.org/10.1038/sdata.2015.35
10. Liu-Helmersson J, Quam M, Wilder-Smith A, Stenlund H, Ebi K, Massad E, Rocklöv J. 2016. Climate change and aedes vectors: 21st century projections for dengue transmission in Europe. EBioMedicine 7:267–277. https://doi.org/10.1016/j.ebiom.2016.03.046
11. Morales D, Ponce P, Cevallos V, Espinosa P, Vaca D, Quezada W. 2019. Resistance status of *Aedes aegypti* to deltamethrin, malathion, and temephos in ecuador. J Am Mosq Control Assoc 35:113–122. https://doi.org/10.2987/19-6831.1
12. Bhatt S, Gething PW, Brady OJ, Messina JP, Farlow AW, Moyes CL, Drake JM, Brownstein JS, Hoen AG, Sankoh O, Myers MF, George DB, Jaenisch T, Wint GRW, Simmons CP, Scott TW, Farrar JJ, Hay SI. 2013. The global distribution and burden of dengue. Nature 496:504–507. https://doi.org/10.1038/nature12060
13. Moreira LA, Iturbe-Ormaetxe I, Jeffery JA, Lu G, Pyke AT, Hedges LM, Rocha BC, Hall-Mendelin S, Day A, Riegler M, Hugo LE, Johnson KN, Kay BH, McGraw EA, van den Hurk AF, Ryan PA, O'Neill SL. 2009. A *Wolbachia* symbiont in *Aedes aegypti* limits infection with dengue, chikungunya, and plasmodium. Cell 139:1268–1278. https://doi.org/10.1016/j.cell.2009.11.042
14. Walker T, Johnson PH, Moreira LA, Iturbe-Ormaetxe I, Frentiu FD, McMeniman CJ, Leong YS, Dong Y, Axford J, Kriesner P, Lloyd AL, Ritchie SA, O'Neill SL, Hoffmann AA. 2011. The wMel *Wolbachia* strain blocks dengue and invades caged *Aedes aegypti* populations. Nature 476:450–453. https://doi.org/10.1038/nature10355
15. Bian G, Xu Y, Lu P, Xie Y, Xi Z. 2010. The endosymbiotic bacterium *Wolbachia* induces resistance to dengue virus in *Aedes aegypti*. PLoS Pathog. 6:e1000833. https://doi.org/10.1371/journal.ppat.1000833
16. Carrington LBet al. 2018. "Field- and clinically derived estimates of *Wolbachia*-mediated blocking of dengue virus transmission potential in *Aedes aegypti* mosquitoes" Proceedings of the National Academy of Sciences, Vol. 115, p 361–366. https://doi.org/10.1073/pnas.1715788115
17. Aliota MT, Walker EC, Uribe Yepes A, Velez ID, Christensen BM, Osorio JE. 2016. The wMel strain of *Wolbachia* reduces transmission of chikungunya virus in *Aedes aegypti*. PLOS Negl Trop Dis 10:e0004677. https://doi.org/10.1371/journal.pntd.0004677
18. Zug R, Hammerstein P. 2012. Still a host of hosts for *Wolbachia*: analysis of recent data suggests that 40% of terrestrial Arthropod species are infected. PLoS ONE 7:e38544. https://doi.org/10.1371/journal.pone.0038544
19. Ross PAet al. 2020. An elusive endosymbiont: does *Wolbachia* occur naturally in *Aedes aegypti?*. Ecology and Evolution 10:1581–1591. https://doi.org/10.1002/ece3.6012
20. Ant TH, Herd CS, Geoghegan V, Hoffmann AA, Sinkins SP. 2018. The *Wolbachia* strain wAu provides highly efficient virus transmission blocking in *Aedes aegypti*. PLOS Pathog. 14:e1006815. https://doi.org/10.1371/journal.ppat.1006815
21. Xi Z, Khoo CCH, Dobson SL. 2005. *Wolbachia* establishment and invasion in an *Aedes aegypti* laboratory population. Science 310:326–328. https://doi.org/10.1126/science.1117607
22. Flores HA, Taneja de Bruyne J, O'Donnell TB, Tuyet Nhu V, Thi Giang N, Thi Xuan Trang H, Thi Thuy Van H, Thi Long V, Thi Dui L, Le Anh Huy H, Thi Le Duyen H, Thi Van Thuy N, Thanh Phong N, Van Vinh Chau N, Thi Hue Kien D, Thuy Vi T, Wills B, O'Neill SL, Simmons CP, Carrington LB. 2020. Multiple *Wolbachia* strains provide comparative levels of protection against dengue virus infection in *Aedes aegypti*. PLOS Pathog. 16:e1008433. https://doi.org/10.1371/journal.ppat.1008433
23. Fraser JE, O'Donnell TB, Duyvestyn JM, O'Neill SL, Simmons CP, Flores HA. 2020. Novel phenotype of *Wolbachia* strain wPip in *Aedes aegypti* challenges assumptions on mechanisms of *Wolbachia*-mediated dengue virus inhibition. PLOS Pathog. 16:e1008410. https://doi.org/10.1371/journal.ppat.1008410
24. Sinkins SP, Braig HR, O'Neill SL. 1995. *Wolbachia* superinfections and the expression of cytoplasmic incompatibility . Proc. R. Soc. Lond. B 261:325–330. https://doi.org/10.1098/rspb.1995.0154

25. Serbus LR, Casper-Lindley C, Landmann F, Sullivan W. 2008. The genetics and cell biology of *Wolbachia* -host interactions. Annu Rev Genet 42:683–707. https://doi.org/10.1146/annurev.genet.41.110306.130354
26. Indriani C, Tantowijoyo W, Rancès E, Andari B, Prabowo E, Yusdi D, Ansari MR, Wardana DS, Supriyati E, Nurhayati I, Ernesia I, Setyawan S, Fitriana I, Arguni E, Amelia Y, Ahmad RA, Jewell NP, Dufault SM, Ryan PA, Green BR, McAdam TF, O'Neill SL, Tanamas SK, Simmons CP, Anders KL, Utarini A. 2020. Reduced dengue incidence following deployments of *Wolbachia*-infected *Aedes aegypti* in Yogyakarta, Indonesia: a quasi-experimental trial using controlled interrupted time series analysis. Gates Open Res 4:50. https://doi.org/10.12688/gatesopenres.13122.1
27. Utarini A, Indriani C, Ahmad RA, Tantowijoyo W, Arguni E, Ansari MR, Supriyati E, Wardana DS, Meitika Y, Ernesia I, Nurhayati I, Prabowo E, Andari B, Green BR, Hodgson L, Cutcher Z, Rancès E, Ryan PA, O'Neill SL, Dufault SM, Tanamas SK, Jewell NP, Anders KL, Simmons CP, AWED Study Group. 2021. Efficacy of *Wolbachia*-infected mosquito deployments for the control of dengue. N Engl J Med 384:2177–2186. https://doi.org/10.1056/NEJMoa2030243
28. Nazni WA, Hoffmann AA, NoorAfizah A, Cheong YL, Mancini MV, Golding N, Kamarul GMR, Arif MAK, Thohir H, NurSyamimi H, ZatilAqmar MZ, NurRuqqayah M, NorSyazwani A, Faiz A, Irfan F-RMN, Rubaaini S, Nuradila N, Nizam NMN, Irwan SM, Endersby-Harshman NM, White VL, Ant TH, Herd CS, Hasnor AH, AbuBakar R, Hapsah DM, Khadijah K, Kamilan D, Lee SC, Paid YM, Fadzilah K, Topek O, Gill BS, Lee HL, Sinkins SP. 2019. Establishment of *Wolbachia* strain wAlbB in malaysian populations of *Aedes aegypti* for dengue control. Curr Biol 29:4241–4248. https://doi.org/10.1016/j.cub.2019.11.007
29. O'Neill SL, Ryan PA, Turley AP, Wilson G, Retzki K, Iturbe-Ormaetxe I, Dong Y, Kenny N, Paton CJ, Ritchie SA, Brown-Kenyon J, Stanford D, Wittmeier N, Anders KL, Simmons CP. 2019. Scaled deployment of *Wolbachia* to protect the community from dengue and other *aedes* transmitted arboviruses. Gates Open Res 2:36. https://doi.org/10.12688/gatesopenres.12844.2
30. Ryan PA, Turley AP, Wilson G, Hurst TP, Retzki K, Brown-Kenyon J, Hodgson L, Kenny N, Cook H, Montgomery BL, Paton CJ, Ritchie SA, Hoffmann AA, Jewell NP, Tanamas SK, Anders KL, Simmons CP, O'Neill SL. 2019. Establishment of wMel *Wolbachia* in *Aedes aegypti* mosquitoes and reduction of local dengue transmission in cairns and surrounding locations in northern Queensland, Australia. Gates Open Res 3:1547. https://doi.org/10.12688/gatesopenres.13061.2
31. Pinto SB, Riback TIS, Sylvestre G, Costa G, Peixoto J, Dias FBS, Tanamas SK, Simmons CP, Dufault SM, Ryan PA, O'Neill SL, Muzzi FC, Kutcher S, Montgomery J, Green BR, Smithyman R, Eppinghaus A, Saraceni V, Durovni B, Anders KL, Moreira LA. 2021. Effectiveness of *Wolbachia*-infected mosquito deployments in reducing the incidence of dengue and other aedes-borne diseases in Niteroi, Brazil: a quasi-experimental study. PLoS Negl Trop Dis 15:e0009556. https://doi.org/10.1371/journal.pntd.0009556
32. Harapan H, Michie A, Sasmono RT, Imrie A. 2020. Dengue: a minireview. Viruses 12:829. https://doi.org/10.3390/v12080829
33. Guzman MG, Gubler DJ, Izquierdo A, Martinez E, Halstead SB. 2016. Dengue infection. Nat Rev Dis Primers 2:16055. https://doi.org/10.1038/nrdp.2016.55
34. van den Elsen K, Quek JP, Luo D. 2021. Molecular insights into the flavivirus replication complex. Viruses 13:956. https://doi.org/10.3390/v13060956
35. Welsch S, Miller S, Romero-Brey I, Merz A, Bleck CKE, Walther P, Fuller SD, Antony C, Krijnse-Locker J, Bartenschlager R. 2009. Composition and three-dimensional architecture of the dengue virus replication and assembly sites. Cell Host & Microbe 5:365–375. https://doi.org/10.1016/j.chom.2009.03.007
36. Eyre NS, Johnson SM, Eltahla AA, Aloi M, Aloia AL, McDevitt CA, Bull RA, Beard MR. 2017. Genome-wide mutagenesis of dengue virus reveals plasticity of the Ns1 protein and enables generation of infectious tagged reporter viruses. J Virol 91:e01455-17. https://doi.org/10.1128/JVI.01455-17
37. Lescar Jet al. 2018. In advances in experimental medicine and biology:115–129.
38. Mackenzie JM, Jones MK, Young PR. 1996. Improved membrane preservation of flavivirus-infected cells with cryosectioning. J Virol Methods 56:67–75. https://doi.org/10.1016/0166-0934(95)01916-2
39. Westaway EG, Mackenzie JM, Kenney MT, Jones MK, Khromykh AA. 1997. Ultrastructure of Kunjin virus-infected cells: colocalization of Ns1 and Ns3 with double-stranded RNA, and of Ns2B with Ns3, in virus-induced membrane structures. J Virol 71:6650–6661. https://doi.org/10.1128/JVI.71.9.6650-6661.1997
40. Amuzu HE, McGraw EA. 2016. *Wolbachia*-based dengue virus inhibition is not tissue-specific in *Aedes aegypti*. PLOS Negl Trop Dis 10:e0005145. https://doi.org/10.1371/journal.pntd.0005145
41. Nainu F, Trenerry A, Johnson KN. 2019. *Wolbachia*-mediated antiviral protection is cell-autonomous. J Gen Virol 100:1587–1592. https://doi.org/10.1099/jgv.0.001342
42. Thomas S, Verma J, Woolfit M, O'Neill SL. 2018. *Wolbachia*-mediated virus blocking in mosquito cells is dependent on Xrn1-mediated viral RNA degradation and influenced by viral replication rate. PLOS Pathog. 14:e1006879. https://doi.org/10.1371/journal.ppat.1006879
43. Bhattacharya T, Newton ILG, Hardy RW. 2020. Viral RNA is a target for *Wolbachia*-mediated pathogen blocking. PLOS Pathog. 16:e1008513. https://doi.org/10.1371/journal.ppat.1008513
44. Caragata EP, Rancès E, Hedges LM, Gofton AW, Johnson KN, O'Neill SL, McGraw EA. 2013. Dietary cholesterol modulates pathogen blocking by *Wolbachia*. PLoS Pathog. 9:e1003459. https://doi.org/10.1371/journal.ppat.1003459
45. Caragata EP, Rancès E, O'Neill SL, McGraw EA. 2014. Competition for amino acids between *Wolbachia* and the mosquito host, *Aedes aegypti*. Microb Ecol 67:205–218. https://doi.org/10.1007/s00248-013-0339-4
46. Cho K-O, Kim G-W, Lee O-K. 2011. *Wolbachia* bacteria reside in host golgi-related Vesicles whose position is regulated by polarity proteins. PLoS ONE 6:e22703. https://doi.org/10.1371/journal.pone.0022703
47. White PMet al. 2017. Reliance of *Wolbachia* on high rates of host proteolysis revealed by a genome-wide Rnai screen of *Drosophila cells*. Genetics 205:1473–1488. https://doi.org/10.1534/genetics.116.198903
48. Manokaran G, Flores HA, Dickson CT, Narayana VK, Kanojia K, Dayalan S, Tull D, McConville MJ, Mackenzie JM, Simmons CP. 2020. Modulation of acyl-carnitines, the broad mechanism behind *Wolbachia* -mediated inhibition of medically important flaviviruses in *Aedes aegypti* . Proc. Natl. Acad. Sci. U.S.A 117:24475–24483. https://doi.org/10.1073/pnas.1914814117
49. Zhang G, Hussain M, O'Neill SL, Asgari S. 2013. *Wolbachia* uses a host microRNA to regulate transcripts of a methyltransferase, contributing to dengue virus inhibition in *Aedes aegypti* . Proc. Natl. Acad. Sci. U.S.A 110:10276–10281. https://doi.org/10.1073/pnas.1303603110
50. Mayoral JG, Etebari K, Hussain M, Khromykh AA, Asgari S. 2014. *Wolbachia* infection modifies the profile, shuttling and structure of microrna in a mosquito cell line. PLoS ONE 9:e96107. https://doi.org/10.1371/journal.pone.0096107
51. Lindsey ARI, Bhattacharya T, Hardy RW, Newton ILG, Hurst GDD, Dubilier N. 2021. *Wolbachia* and virus alter the host transcriptome at the interface of nucleotide metabolism pathways. mBio 12. https://doi.org/10.1128/mBio.03472-20
52. Bhattacharya T, Yan L, Crawford JM, Zaher H, Newton ILG, Hardy RW. 2022. Differential viral RNA methylation contributes to pathogen blocking in *Wolbachia*-colonized arthropods. PLoS Pathog 18:e1010393. https://doi.org/10.1371/journal.ppat.1010393
53. Rancès E, Ye YH, Woolfit M, McGraw EA, O'Neill SL. 2012. The relative importance of innate immune priming in *Wolbachia*-mediated dengue interference. PLoS Pathog 8:e1002548. https://doi.org/10.1371/journal.ppat.1002548
54. Pan X, Zhou G, Wu J, Bian G, Lu P, Raikhel AS, Xi Z. 2012. *Wolbachia* induces reactive oxygen species (ROS)-dependent activation of the toll pathway to control dengue virus in the mosquito *Aedes aegypti*. Proc Natl Acad Sci U S A 109:E23–31. https://doi.org/10.1073/pnas.1116932108
55. Fraser JE, De Bruyne JT, Iturbe-Ormaetxe I, Stepnell J, Burns RL, Flores HA, O'Neill SL. 2017. Novel *Wolbachia*-transinfected *Aedes aegypti* mosquitoes possess diverse fitness and vector competence phenotypes. PLOS Pathog. 13:e1006751. https://doi.org/10.1371/journal.ppat.1006751
56. McLean BJ, Dainty KR, Flores HA, O'Neill SL. 2019. Differential suppression of persistent insect specific viruses in Trans-infected wMel and wMelPop-CLA Aedes-derived mosquito lines. Virology 527:141–145. https://doi.org/10.1016/j.virol.2018.11.012

57. Fattouh N, Cazevieille C, Landmann F. 2019. *Wolbachia* endosymbionts subvert the endoplasmic reticulum to acquire host membranes without triggering ER stress. PLOS Negl Trop Dis 13:e0007218. https://doi.org/10.1371/journal.pntd.0007218
58. McMeniman CJ, Lane AM, Fong AWC, Voronin DA, Iturbe-Ormaetxe I, Yamada R, McGraw EA, O'Neill SL. 2008. Host adaptation of a *Wolbachia* strain after long-term serial passage in mosquito cell lines. Appl Environ Microbiol 74:6963–6969. https://doi.org/10.1128/AEM.01038-08
59. Casper-Lindley C, Kimura S, Saxton DS, Essaw Y, Simpson I, Tan V, Sullivan W. 2011. Rapid fluorescence-based screening for *Wolbachia* endosymbionts in drosophila germ line and somatic tissues. Appl Environ Microbiol 77:4788–4794. https://doi.org/10.1128/AEM.00215-11
60. Guzman MG, Harris E. 2015. Dengue. The Lancet 385:453–465. https://doi.org/10.1016/S0140-6736(14)60572-9
61. Barletta ABF, Alves LR, Silva MCLN, Sim S, Dimopoulos G, Liechocki S, Maya-Monteiro CM, Sorgine MHF. 2016. Emerging role of lipid droplets in *Aedes aegypti* immune response against bacteria and dengue virus. Sci Rep 6:19928. https://doi.org/10.1038/srep19928
62. Monson EA, Crosse KM, Duan M, Chen W, O'Shea RD, Wakim LM, Carr JM, Whelan DR, Helbig KJ. 2021. Intracellular lipid droplet accumulation occurs early following viral infection and is required for an efficient interferon response. Nat Commun 12:4303. https://doi.org/10.1038/s41467-021-24632-5
63. Olzmann JA, Carvalho P. 2019. Dynamics and functions of lipid droplets. Nat Rev Mol Cell Biol 20:137–155. https://doi.org/10.1038/s41580-018-0085-z
64. Tang W-C, Lin R-J, Liao C-L, Lin Y-L. 2014. Rab18 facilitates Dengue virus infection by targeting fatty acid synthase to sites of viral replication. J Virol 88:6793–6804. https://doi.org/10.1128/JVI.00045-14
65. Junjhon J, Pennington JG, Edwards TJ, Perera R, Lanman J, Kuhn RJ. 2014. Ultrastructural characterization and three-dimensional architecture of replication sites in dengue virus-infected mosquito cells. J Virol 88:4687–4697. https://doi.org/10.1128/JVI.00118-14
66. Samsa MM, Mondotte JA, Iglesias NG, Assunção-Miranda I, Barbosa-Lima G, Da Poian AT, Bozza PT, Gamarnik AV. 2009. Dengue virus capsid protein USURPS lipid droplets for viral particle formation. PLoS Pathog. 5:e1000632. https://doi.org/10.1371/journal.ppat.1000632
67. Molloy JC, Sommer U, Viant MR, Sinkins SP. 2016. *Wolbachia* modulates lipid metabolism in *Aedes albopictus* mosquito cells. Appl Environ Microbiol 82:3109–3120. https://doi.org/10.1128/AEM.00275-16
68. Ponton F, Wilson K, Holmes A, Raubenheimer D, Robinson KL, Simpson SJ. 2015. Macronutrients mediate the functional relationship between *Drosophila* and *Wolbachia*. Proc Biol Sci 282:20142029. https://doi.org/10.1098/rspb.2014.2029
69. Koh C, Islam MN, Ye YH, Chotiwan N, Graham B, Belisle JT, Kouremenos KA, Dayalan S, Tull DL, Klatt S, Perera R, McGraw EA. 2020. Dengue virus dominates lipid metabolism modulations in *Wolbachia*-coinfected *Aedes aegypti*. Commun Biol 3:518. https://doi.org/10.1038/s42003-020-01254-z
70. Heier C, Kühnlein RP. 2018. Triacylglycerol metabolism in drosophila melanogaster Genetics 210:1163–1184. https://doi.org/10.1534/genetics.118.301583
71. Chirala SS, Wakil SJ. 2004. Structure and function of animal fatty acid synthase. Lipids 39:1045–1053. https://doi.org/10.1007/s11745-004-1329-9
72. O'Neill SL, Ryan PA, Turley AP, Wilson G, Retzki K, Iturbe-Ormaetxe I, Dong Y, Kenny N, Paton CJ, Ritchie SA, Brown-Kenyon J, Stanford D, Wittmeier N, Jewell NP, Tanamas SK, Anders KL, Simmons CP. 2019. Scaled deployment of *Wolbachia* to protect the community from dengue and other *Aedes* transmitted Arboviruses. Gates Open Res 2:36. https://doi.org/10.12688/gatesopenres.12844.3
73. Pinto SB, Riback TIS, Sylvestre G, Costa G, Peixoto J, Dias FBS, Tanamas SK, Simmons CP, Dufault SM, Ryan PA, O'Neill SL, Muzzi FC, Kutcher S, Montgomery J, Green BR, Smithyman R, Eppinghaus A, Saraceni V, Durovni B, Anders KL, Moreira LA. 2021. Effectiveness of *Wolbachia*-infected mosquito deployments in reducing the incidence of dengue and other aedes-borne diseases in niterói, Brazil: a quasi-experimental study. PLOS Negl Trop Dis 15:e0009556. https://doi.org/10.1371/journal.pntd.0009556
74. World Health Organization. 2021. Thirteenth meeting of the WHO vector control advisory group. Available from: https://www.who.int/publications/i/item/9789240021792
75. Baldo L, Dunning Hotopp JC, Jolley KA, Bordenstein SR, Biber SA, Choudhury RR, Hayashi C, Maiden MCJ, Tettelin H, Werren JH. 2006. Multilocus sequence typing system for the endosymbiont *Wolbachia* pipientis. Appl Environ Microbiol 72:7098–7110. https://doi.org/10.1128/AEM.00731-06
76. Landmann F. 2019. The *Wolbachia* endosymbionts. Microbiol Spectr 7. https://doi.org/10.1128/microbiolspec.BAI-0018-2019
77. Wu M, Sun LV, Vamathevan J, Riegler M, Deboy R, Brownlie JC, McGraw EA, Martin W, Esser C, Ahmadinejad N, Wiegand C, Madupu R, Beanan MJ, Brinkac LM, Daugherty SC, Durkin AS, Kolonay JF, Nelson WC, Mohamoud Y, Lee P, Berry K, Young MB, Utterback T, Weidman J, Nierman WC, Paulsen IT, Nelson KE, Tettelin H, O'Neill SL, Eisen JA. 2004. Phylogenomics of the reproductive parasite *Wolbachia* pipientis wMel: a streamlined genome overrun by mobile genetic elements. PLoS Biol. 2:E69. https://doi.org/10.1371/journal.pbio.0020069
78. Ant TH, Mancini MV, McNamara CJ, Rainey SM, Sinkins SP. 2023. *Wolbachia*-virus interactions and arbovirus control through population replacement in mosquitoes. Pathog Glob Health 117:245–258. https://doi.org/10.1080/20477724.2022.2117939
79. Lin M, Rikihisa Y. 2003. Ehrlichia chaffeensis and anaplasma phagocytophilum lack genes for lipid A biosynthesis and incorporate cholesterol for their survival. Infect Immun 71:5324–5331. https://doi.org/10.1128/IAI.71.9.5324-5331.2003
80. Fraser JE, O'Donnell TB, Duyvestyn JM, O'Neill SL, Simmons CP, Flores HA. 2020. Novel phenotype of *Wolbachia* strain wPip in *Aedes aegypti* challenges assumptions on mechanisms of *Wolbachia*-mediated dengue virus inhibition. PLoS Pathog 16:e1008410. https://doi.org/10.1371/journal.ppat.1008410
81. Monson EA, Trenerry AM, Laws JL, Mackenzie JM, Helbig KJ. 2021. Lipid droplets and lipid mediators in viral infection and immunity. FEMS Microbiol Rev 45:fuaa066. https://doi.org/10.1093/femsre/fuaa066
82. Heaton NS, Perera R, Berger KL, Khadka S, LaCount DJ, Kuhn RJ, Randall G. 2010. Dengue virus nonstructural protein 3 redistributes fatty acid synthase to sites of viral replication and increases cellular fatty acid synthesis. Proc. Natl. Acad. Sci. U.S.A 107:17345–17350. https://doi.org/10.1073/pnas.1010811107
83. Perera R, Riley C, Isaac G, Hopf-Jannasch AS, Moore RJ, Weitz KW, Pasa-Tolic L, Metz TO, Adamec J, Kuhn RJ. 2012. Dengue virus infection perturbs lipid homeostasis in infected mosquito cells. PLoS Pathog. 8:e1002584. https://doi.org/10.1371/journal.ppat.1002584
84. Hitakarun A, Williamson MK, Yimpring N, Sornjai W, Wikan N, Arthur CJ, Pompon J, Davidson AD, Smith DR. 2022. Cell type variability in the incorporation of lipids in the dengue virus Virion. Viruses 14:2566. https://doi.org/10.3390/v14112566
85. Carro AC, Damonte EB. 2013. Requirement of cholesterol in the viral envelope for dengue virus infection. Virus Res 174:78–87. https://doi.org/10.1016/j.virusres.2013.03.005
86. Monson EA, Crosse KM, Das M, Helbig KJ. 2018. Lipid droplet density alters the early innate immune response to viral infection. PLOS ONE 13:e0190597. https://doi.org/10.1371/journal.pone.0190597
87. Monson EA, Whelan DR, Helbig KJ. 2021. Lipid droplet motility increases following viral immune stimulation. Int J Mol Sci 22:4418. https://doi.org/10.3390/ijms22094418
88. Geoghegan V, Stainton K, Rainey SM, Ant TH, Dowle AA, Larson T, Hester S, Charles PD, Thomas B, Sinkins SP. 2017. Perturbed cholesterol and vesicular trafficking associated with dengue blocking in *Wolbachia*-infected *Aedes aegypti* cells. Nat Commun 8:526. https://doi.org/10.1038/s41467-017-00610-8
89. Rainey SM, Geoghegan V, Lefteri DA, Ant TH, Martinez J, McNamara CJ, Kamel W, de Laurent ZR, Castello A, Sinkins SP. 2023. Differences in proteome perturbations caused by the *Wolbachia* strain wAu suggest multiple mechanisms of *Wolbachia*-mediated antiviral activity. Sci Rep 13:11737. https://doi.org/10.1038/s41598-023-38127-4
90. Heaton NS, Randall G. 2010. Dengue virus-induced autophagy regulates lipid metabolism. Cell Host & Microbe 8:422–432. https://doi.org/10.1016/j.chom.2010.10.006
91. Thiele C, Penno A. 2016. Lipid droplets. Encyclopedia of Cell Biology:273–278. https://doi.org/10.1016/B978-0-12-394447-4.20023

92. Gao M, Huang X, Song B-L, Yang H. 2019. The biogenesis of lipid droplets: lipids take center stage. Progress in Lipid Research 75:100989. https://doi.org/10.1016/j.plipres.2019.100989
93. Zaitseva E, Yang S-T, Melikov K, Pourmal S, Chernomordik LV. 2010. Dengue virus ensures its fusion in late endosomes using compartment-specific lipids. PLoS Pathog. 6:e1001131. https://doi.org/10.1371/journal.ppat.1001131
94. Kielian M, Chanel-Vos C, Liao M. 2010. Alphavirus entry and membrane fusion. Viruses 2:796–825. https://doi.org/10.3390/v2040796
95. Fraser JE, De Bruyne JT, Iturbe-Ormaetxe I, Stepnell J, Burns RL, Flores HA, O'Neill SL. 2017. Novel *Wolbachia*-transinfected *Aedes aegypti* mosquitoes possess diverse fitness and vector competence phenotypes. PLoS Pathog 13:e1006751. https://doi.org/10.1371/journal.ppat.1006751
96. Livak KJ, Schmittgen TD. 2001. Analysis of relative gene expression data using real-time quantitative PCR and the 2(-Delta Delta C(T)) method. Methods 25:402–408. https://doi.org/10.1006/meth.2001.1262
97. O'Brien CA, Hobson-Peters J, Yam AWY, Colmant AMG, McLean BJ, Prow NA, Watterson D, Hall-Mendelin S, Warrilow D, Ng M-L, Khromykh AA, Hall RA. 2015. Viral RNA intermediates as targets for detection and discovery of novel and emerging mosquito-borne viruses. PLOS Negl Trop Dis 9:e0003629. https://doi.org/10.1371/journal.pntd.0003629
98. Lee E, Hien Nguyen T, Yen Nguyen T, Nam Vu S, Duong Tran N, Trung Nghia L, Mai Vien Q, Dong Nguyen T, Kriiger Loterio R, Iturbe-Ormaetxe I, Flores HA, O'Neill SL, Anh Dang D, Simmons CP, Fraser JE. 2022. Transient Introgression of *Wolbachia* into *Aedes aegypti* populations does not elicit an antibody response to *Wolbachia* surface protein in community members. Pathogens 11:535. https://doi.org/10.3390/pathogens11050535
99. Gentry MK, Henchal EA, McCown JM, Brandt WE, Dalrymple JM. 1982. Identification of distinct antigenic determinants on dengue-2 virus using monoclonal antibodies. Am J Trop Med Hyg 31:548–555. https://doi.org/10.4269/ajtmh.1982.31.548
100. Reed LJ, Muench H. 1938. A simple method of estimating fifty per cent endpoints. Am J Epidemiol 27:493–497. https://doi.org/10.1093/oxfordjournals.aje.a118408
101. Kremer JR, Mastronarde DN, McIntosh JR. 1996. Computer visualization of three-dimensional image data using IMOD. J Struct Biol 116:71–76. https://doi.org/10.1006/jsbi.1996.0013